# Inception of gravel bed motion beneath tidal bores: an experimental study.

N. Khezri[1] and H. Chanson[1]
[1]School of civil engineering
University of Queensland
QLD 4067
AUSTRALIA
E-mail: h.chanson@uq.edu.au

***Abstract:*** *A tidal bore is a positive surge taking place during the flood tide under macro-tidal conditions and the bore represents the leading edge of the tidal wave propagating upstream. The fundamentals of tidal bores remain unknown, although some physical experiments were performed during the last two decades. In this study, some physical modelling was performed to investigate the tidal bore propagation and turbulent mixing on fixed and movable gravel beds with both undular and breaking bores. Further observations of particle motion beneath the bore front were recorded. The results showed the significant impact of breaking bore propagation on the gravel bed motion, associated with upstream gravel bed load motion behind the bore. The gravel bed particles were de-stabilised by the roller toe passage and advected upstream with a convective velocity about 1/7th of the bore celerity.*

***Keywords:*** *Tidal bores, Turbulence, Sediment motion, Inception, Gravel bed, Physical modelling.*

## 1. INTRODUCTION

A tidal bore is a natural phenomenon with significant ecological impacts on the estuarine system (Donnelley and Chanson, 2005; Chanson, 2011). A bore may result from a combination of several parameters including the tidal conditions, bathymetry, river mouth shape and etc. (Darwin 1897). Some famous tidal bores are those of Qiantang River (China), Amazon River (Brazil) and Seine River (France). A tidal bore may form in a narrow funnelled channel mouth during the early flood tide under spring tide conditions. The positive surge propagates upstream. The bore propagation induces some enhanced, turbulent mixing resulting in bed erosion and upstream sediment advection (Chen et al., 1990; Tessier and Terwindt, 1994; Koch and Chanson, 2009).

In this study, the turbulent mixing characteristics of breaking and undular tidal bores were investigated physically including in terms of sediment motion on a movable gravel bed. The experimental study was based upon a Froude dynamic similarity, and some detailed velocity measurements were conducted for a number of Froude Numbers to provide some Eulerian description of the turbulent flow field. Some sediment tracking under both breaking and undular bores brought some Lagrangian understanding of turbulent mixing and bed load motion beneath the tidal bore front.

## 2. EXPERIMENTAL SETUP & INSTRUMENTATION

The experiments were performed in a rectangular channel, 0.5 m wide and 12 m long, made of smooth PVC bed and glass walls. A fast closing tainter gate was located at x=11.5 m downstream of the channel upstream end. The tainter gate could be closed rapidly, completely or partially, to generate the tidal bore propagation upstream into the channel.

Two orifice meters, designed based on British Standards (British Standard 1943), were used to record the initially steady discharge. The steady flow depths were measured using rail mounted pointer gauges. Some acoustic displacement meters Microsonic™ Mic+25/IU/TC were installed between x=4 to 10.8 m above the water surface to detect the water elevation fluctuations. An acoustic Doppler velocimeter (ADV) Nortek™ Vectrino+ was also installed at x=5 m to measure the turbulent velocity fluctuations. The ADV system was equipped with a three-dimensional side looking head. During all experiments, the observations were conducted between x=4 to 6 m and some video movies were recorded with a digital video camera Panasonic™ NV-GS300 (25 fps).

For all the experiments, the PVC bed was covered with a series of plywood sheets, 1.2 m long and 0.5 m wide, covered by natural blue granite gravels (density 2.65) which were sieved between 4.75 mm and 6.70 mm, glued in resin and covered by a spray gloss surface finish. The setup was called the fixed gravel bed configuration. For the second setup, a 1 m long section of smooth-painted plywood sheet was installed beneath the study region and a layer of loose gravels was spread evenly prior to the beginning of each experiment. For the movable bed configuration, some video movies of the gravel bed motion were recorded.

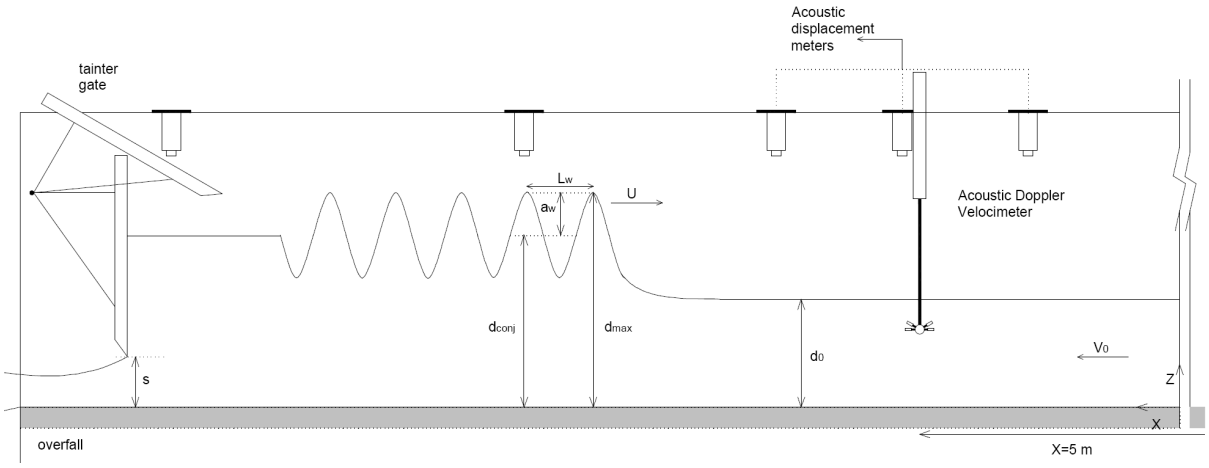


**Figure 1 Sketch of the channel test section and upstream bore propagation**

### 2.1. Experimental flow conditions and tidal bore generation

The experiments were conducted with the same initially steady water discharge: Q=0.05 $m^3$/s and initial water depth $d_o$=0.136 m. The initial flow conditions were identical for both fixed and movable gravel bed configurations.

The generation of the tidal bore was performed by the rapid closure of the tainter gate. After closure, the underflow gate opening ranged 0 to 100 mm. By changing this opening, both breaking and undular bores could be generated with the same identical initial flow conditions. After the gate closure, the tidal bore moved upstream, the acoustic displacement meters sampled non-intrusively the water surface elevation along the channel centreline, and the ADV sampling volume was located on the channel centreline at x=5 m where x is the longitudinal distance from the channel upstream end positive downstream. For each experiment, the data acquisition was started 60 s prior to the tidal bore generation. The gate closure took place in 0.1 to 0.15 s. Each experiment was stopped once the bore reached the channel upstream end. Note that the gate was similar to that used by Koch and Chanson (2009) and Docherty and Chanson (2010).

## 3. BASIC RESULTS

The water surface measurements and visual observations were conducted for fixed and movable bed configurations with similar initial conditions (Q=0.05$m^3$/s, $d_o$=0.136m) and a range of Froude numbers Fr, where Fr is defined as Fr=($V_o$+U)/$\sqrt{gd_o}$ with $V_0$ the initial flow velocity positive downstream, U the bore front velocity positive upstream, and g the gravity acceleration. At the larger Froude numbers (Fr>1.3 to 1.4), a bore with a breaking roller was observed. The bore had a marked quasi-two-dimensional roller. Undular bores were observed for the smaller Froude numbers (Fr<1.3). For Froude numbers between 1.2 and 1.3, some slight breaking was observed at the first wave crest.

The experiments were conducted in both undular and breaking tidal bores on fixed and mobile beds. The data from acoustic displacement meter and acoustic Doppler Velocimeter (ADV) were used to perform steady and unsteady analyses. The ADV data were post-processed in WinADV. In steady flows, some phase-space threshold despiking and the removal of communication errors, low SNRs and low correlations were performed. For the unsteady flows, only the removal of communication errors and a replacement by linear interpolation were conducted since the other forms of post-

processing were never validated in highly-unsteady flows. Table 1 summarises the experimental flow conditions for the turbulent velocity measurements and particle tracking experiments (mobile bed only). For the undular bores, Table 1 lists further the relative wave amplitude $a_w/d_o$ and wave steepness $a_w/L_w$. Note that the water depths were measured above the top of the gravel bed using a semi-circular footing with a 25.1 cm$^2$ area.

**Table 1 Experimental flow conditions for turbulent measurements**

| Bed configuration | Gate opening (mm) | Q ($m^3/s$) | $d_o$ (m) | $V_o$ (m/s) | U (m/s) | $Z/d_o$ | Fr | Bore type | $d_{conj}/d_o$ | $d_{max}/d_o$ | $a_w/d_o$ | $a_w/L_w$ |
|---|---|---|---|---|---|---|---|---|---|---|---|---|
| **Fixed Bed** | 0 | 0.050 | 0.136 | 0.74 | 0.87 | 0.613 | 1.39 | Breaking | 1.63 | N/A | N/A | N/A |
| | 60 | 0.052 | 0.136 | 0.76 | 0.63 | 0.605 | 1.19 | Undular | 1.28 | 1.49 | 0.178 | 0.026 |
| **Mobile Bed** | 0 | 0.051 | 0.136 | 0.75 | 0.87 | 0.613 | 1.40 | Breaking | 1.64 | N/A | N/A | N/A |
| | 60 | 0.050 | 0.136 | 0.74 | 0.61 | 0.613 | 1.17 | Undular | 1.30 | 1.51 | 0.167 | 0.025 |

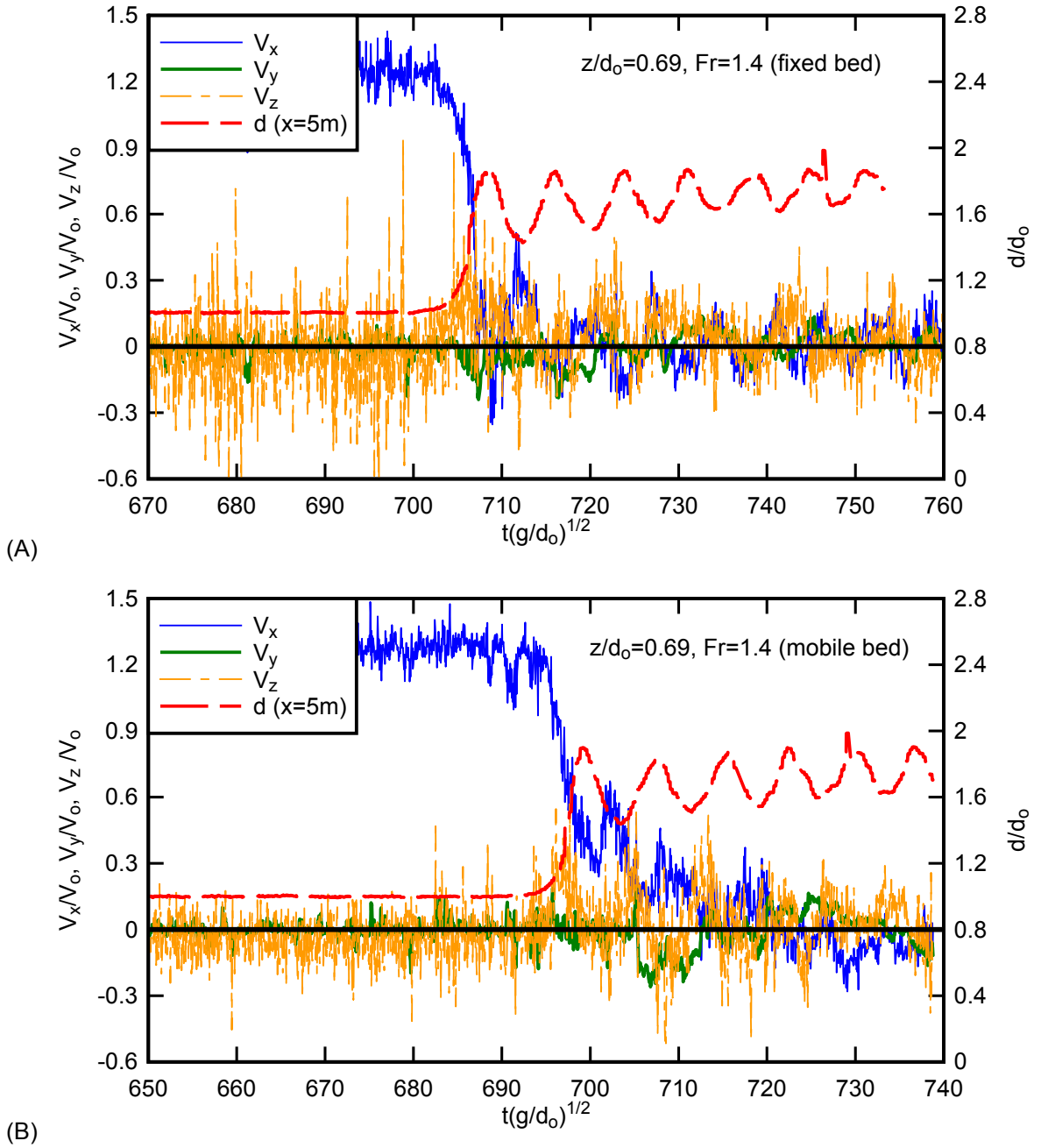


**Figure 2 Instantaneous turbulent velocities in a breaking tidal bore on (A) fixed and (B) mobile bed configurations - Q = 0.05 $m^3/s$, $d_o$= 0.136 m, U = 0.87 m/s, Fr =1.4**

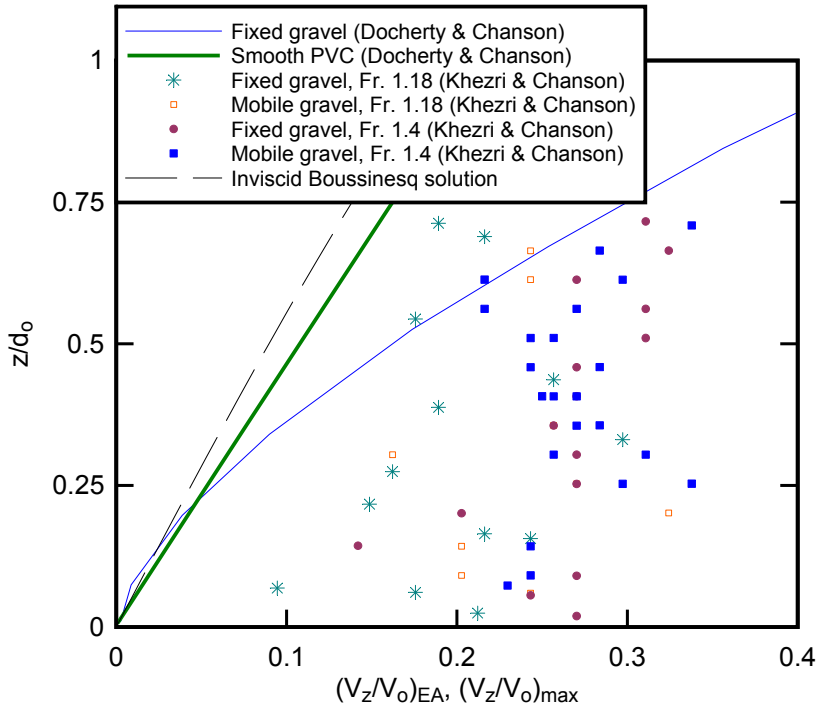


**Figure 3 Maximum instantaneous vertical velocity beneath the tidal bore roller and corresponding free-surface vertical velocity on mobile and fixed gravel beds - Comparison with the ensemble-averaged data of Docherty and Chanson (2010) and an inviscid Boussinesq equation solution calculated from the measured free-surface profile**

Figure 2 presents some typical results in terms of the water elevation above the bed and turbulent velocity components. Both graphs were obtained for a similar Froude number Fr at same relative elevation $z/d_o$ but for the two types of bed configurations. Herein $V_x$, $V_y$ and $V_z$ were respectively positive downstream, towards the left sidewall and upwards. The propagation of the bore front was associated with a rapid rise of the water surface during the breaking roller passage followed by some residual undulations for Fr = 1.4. The propagation of the bore roller was linked with some strong longitudinal deceleration and some positive instantaneous vertical velocities as reported by Hornung et al. (1995) and Koch and Chanson (2009). The former effect is clearly seen in Figure 2, while the latter is illustrated in Figure 3. Figure 3 presents the maximum instantaneous vertical velocities at several relative vertical elevations $z/d_0$ for two Froude numbers. Both fixed and mobile bed configuration data are shown. The results are compared to the ensemble-averaged data of Docherty and Chanson (2010) and an inviscid solution of the Boussinesq equation calculated from the observed free-surface curvature immediately upstream of the roller (Montes and Chanson, 1998). The general trend was consistent and emphasised the existence of an upward momentum flux during the bore front passage (Fig. 3).

The experimental data showed also the existence of a transient recirculation next to the bed: that is, the longitudinal flow deceleration ended with a negative longitudinal velocity component $V_x < 0$. Further the results showed that, for the same Froude number and same relative elevation $z/d_0$, the longitudinal velocity on mobile bed did not reach the maximum instantaneous negative velocities observed on the fixed bed. This could be linked to some energy dissipation in the form of energy transfer to move the gravel particles behind the bore. Indeed the passage of the bore was associated with some upstream gravel bed motion (Section 4). Close to the bed, the negative transient recirculation velocities were large with both mobile and fixed bed configurations, and significantly larger than those observed on smooth bed (Koch and Chanson, 2009). The findings were consistent with the data of Docherty and Chanson (2010). They tended to imply that the transient recirculation was strongly linked to the boundary friction, as shown by recent numerical results (Lubin et al., 2010; Furuyama and Chanson, 2010). Some large vertical velocity fluctuations were observed shortly after the bore passage. The data showed the time required for the development of vortical structures.

## 4. BED LOAD MOTION

During the mobile gravel bed experiments, the sediment particles were tracked and their motion was recorded with the video-camera. About 15 to 20 video movies were made for each tidal bore experiment. For each video recording, 15 to 20 particles were tracked typically. Figure 4(A) shows a sample of initial positions of the coloured tracked sediments. The particle motion relative to the tidal bore propagation was compared with three characteristic points of the bore free-surface (Fig. 4(B)). These were (1) the start of the upward free-surface curvature (Point 1, Fig. 4(B)), (2) the toe of the bore roller (Point 2, Fig. 4(B)) and (3) the conjugate depth (Point 3, Fig. 4(B)). For the experiment shown in Figures 4(A) and 4(B), Figure 5(A) presents the results for the bed load motion and gravel particle motion and Figure 5(B) shows another run and set of results. In Figure 5, the horizontal axis represents 0.50 m and X is positive upstream: that is, a particle motion towards the right side of the images in Figures 4(A) and 4(B). The motion of the sediment particles, named A to Q (Fig. 4(A)), is presented and compared with propagation of the 3 characteristic points of the bore free-surface in Figure 5(A).

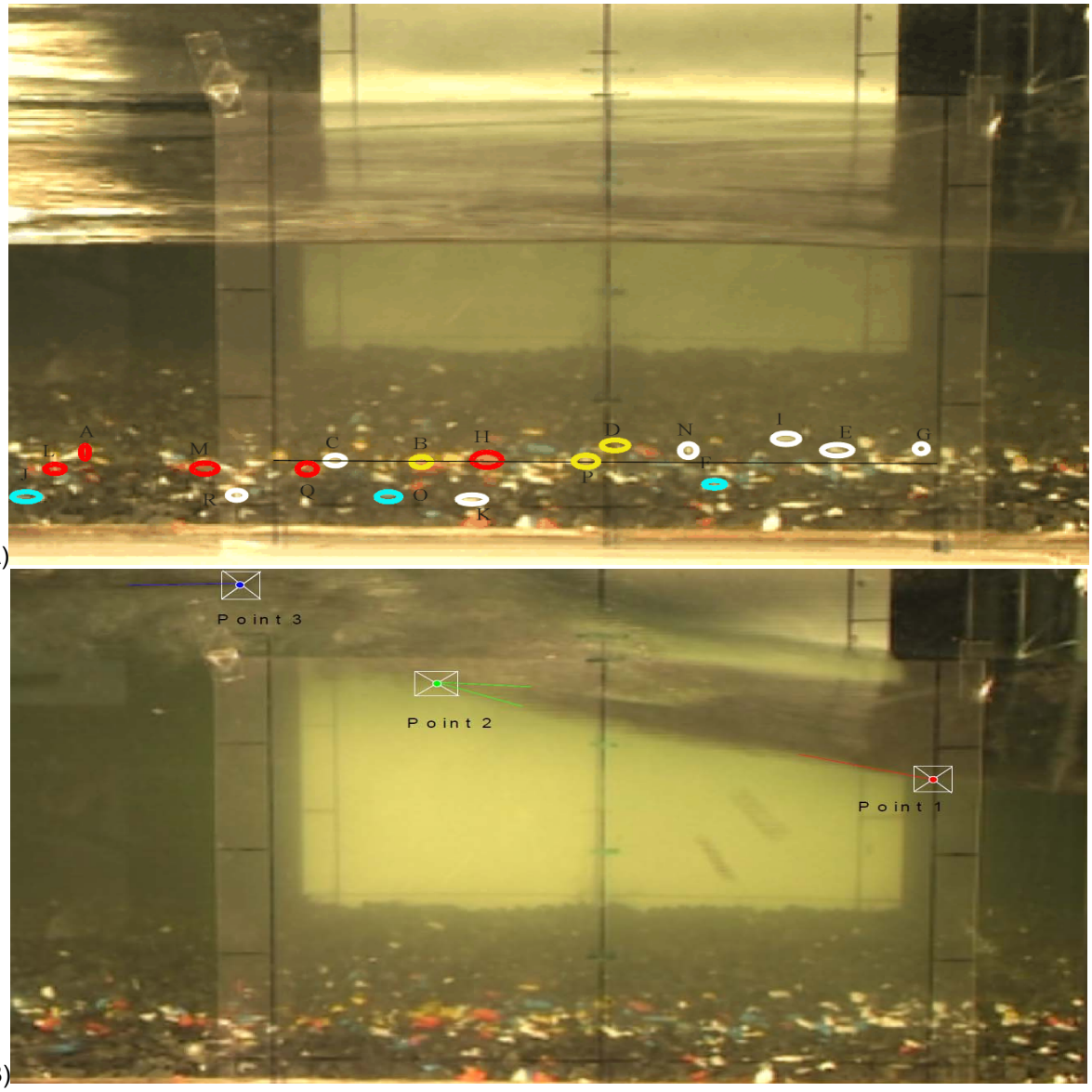


**Figure 4 Bed load particle tracking. (A) Initial location of particles (layout) before the bore arrival. (B) Definition of Points 1, 2 & 3 - Q = 0.051 $m^3$/s, movable gravel bed, Fr = 1.4, Gate opening: h=0, Run 13**

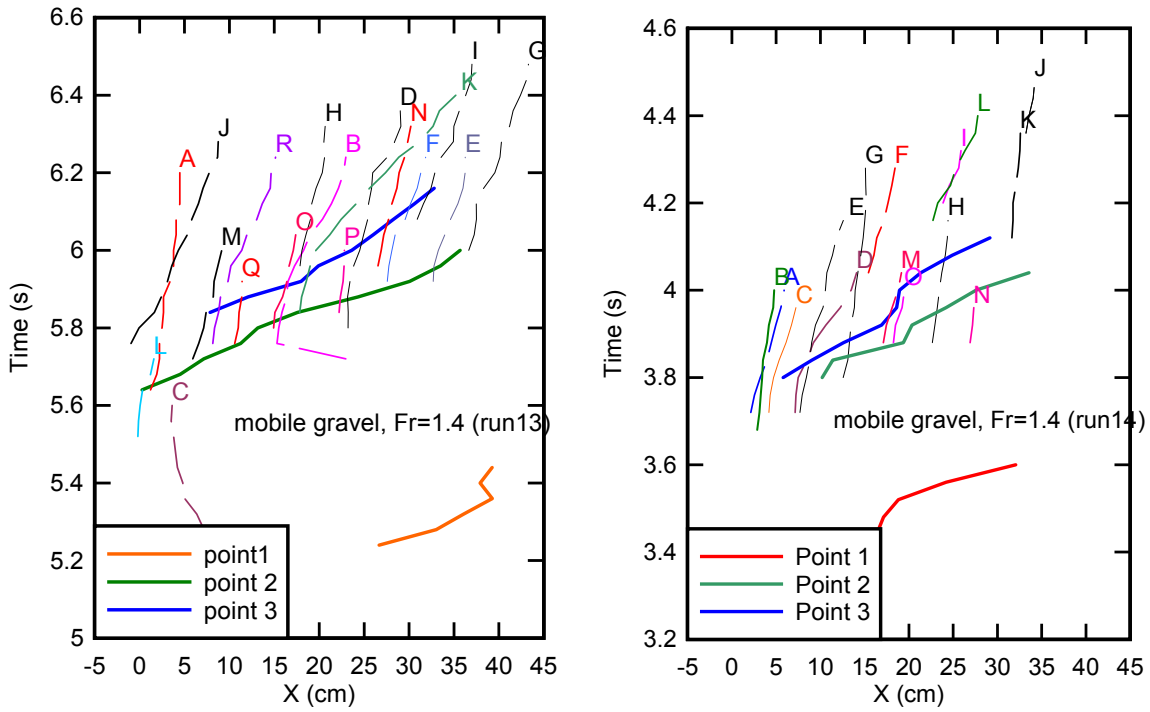


**Figure 5 Gravel particle trajectories and bore propagation as functions of time - Q = 0.051 m$^3$/s, movable gravel bed, Fr = 1.4, Gate opening: h=0, (A) Run 13 (B) Run 14**

### 4.1. Results

Prior to the tidal bore, no gravel bed motion was observed. For the undular bore experiment (Fr=1.17), the sediment movement was negligible. During each video, at most two sediment particles would move shortly, typically for less than 0.1 s. That is, this was mostly some form of particle rotation rather than a change of absolute position. During the breaking tidal bore (Fr=1.4), at least 15 to 20 gravel trajectories were easily tracked for at least 0.2 s in each video. (These were the coloured particles seen in Figure 4 that were initially laid down along a 5 cm wide strip and surrounded by non-coloured particles.) Figure 5 presents some typical results. The total number of particles in motion was much larger in each video movie, but only particle within the depth of field of the camera lens were tracked (Fig. 4(A)).

### 4.2. Discussion

The physical data demonstrated the strong gravel bed load motion during the breaking bore propagation. Physically, for a particle initially fixed on the bed, the propagation of the breaking bore was associated with a combination of several de-stabilising processes including some transient upward irrotational velocity linked with ideal fluid flow motion, a highly turbulent motion and a pressure wave. For the irrotational flow motion, the free-surface is a streamline and the upstream bore propagation is characterised by an upward streamline curvature, hence a rapid pressure and velocity redistributions including a transient positive vertical velocity (Fig. 3). Turbulence shear contributes further to a drag force acting in the upstream direction during the transient recirculation seen in Figure 2A. More the larger flow depth behind the bore implies a positive pressure gradient $\partial P/\partial x$ close to the bed that is proportional to:

$$\partial P/\partial x \propto \rho\, g\, (d_{conj} - d_o) \propto (Fr - 1) \quad (1)$$

All these processes add together and contribute to the gravel bed load inception and upstream advection of gravel particles.

The present observations highlighted that the gravel bed load motion was initiated primarily by the passage of the roller toe (e.g. Fig. 5). The finding would tend to support the predominant roles of the highly turbulent motion beneath the tidal bore roller and the effects of the unsteady pressure gradient $\partial P/\partial x$. The former effect was documented numerically by Lubin et al. (2010) showing the generation of large scale vortices beneath the breaking bore front and their advection behind the bore front. The latter effect was discussed by Lighthill (1978), but both theoretical and numerical approaches lacked physical validation data until now.

## 5. CONCLUSION

In this physical study, the turbulent characteristics beneath both undular and breaking bore were investigated. The experiments were conducted on two types of rough gravel bed (fixed and movable). Some complementary instruments (displacement meters, ADV, video camera) were used to record the key characteristics of the unsteady turbulent flow motion during tidal bore propagation and its impact in terms of gravel sediment transport.

The velocity measurements at different vertical elevations were performed using acoustic Doppler velocimetry with high temporal resolution (200 Hz). The data showed some basic differences under undular and breaking bores on fixed and movable gravel bed configurations. With a breaking bore, the turbulent velocity data indicated that, with similar initial flow conditions and relative elevation (Fr, $z/d_o$), the magnitude of negative transient longitudinal velocity close to the bed was greater on fixed bed than on mobile bed. This was explained as a result of energy dissipation and transfer to set into motion the gravel bed material. The negative transient recirculation velocities were however large close to the bed, highlighting the effect of boundary friction. The propagation of the breaking bore highlighted some instantaneous upwards momentum flux linked with the streamline curvature immediately upstream of the roller.

The physical study showed that the undular bore had a negligible effect on gravel particle movement, while a large amount of gravel particles were set into motion beneath the breaking bore front and advected upstream. The data showed an intense gravel bed motion under the breaking bore. The gravel particles were de-stabilised by the roller toe passage (Point 2, Fig. 4(B)) and advected upstream with a convective velocity about 1/7th of the bore celerity. The results hinted the predominant roles of the highly turbulent motion beneath the tidal bore roller and the effects of the unsteady pressure gradient $\partial P/\partial x$.

It is known that the tidal bore propagation does have a major impact on the sediment processes in the estuarine zone. It is believed that the present investigation is the first physical study into the bed load motion under tidal bores and future contributions on this topic would provide further details into the flow physics with other particle characteristics including different granulometry and density.

## 6. ACKNOWLEDGEMENTS

The first author acknowledges the technical assistance of Ahmed Ibrahim, Graham Illidge and Clive Booth (The University of Queensland).

## 7. REFERENCES

British Standards (1943). *Flow measurement*. British Standard Code BS 1042:1943, British Standard Institution. London.

Chanson, H. (2011). *Tidal Bores, Aegir, Eagre, Mascaret, Pororoca*. World Scientific, Singapore, 2011.

Chen, J., Liu, C., Zhang, C., and Walker, H.J. (1990). *Geomorphological Development and Sedimentation in Qiantang Estuary and Hangzhou Bay*. Journal of Coastal Research, Vol. 6, No. 3, pp. 559-572.

Darwin, G.H. (1897). *The Tides and Kindred Phenomena in the Solar System*. Lectures delivered at the Lowell Institute, Boston, W.H. Freeman and Co. Publ., London, 1962.

Docherty, N., and Chanson, H. (2010). *Characterisation of Unsteady Turbulence in Breaking Tidal Bores including the Effects of Bed Roughness*. Hydraulic Model Report No. CH76/10, School of Civil Engineering, The University of Queensland, Brisbane, Australia, 112 pages

Donnelly, C., and Chanson, H. (2005). *Environmental impact of undular tidal bores in tropical rivers*. Environmental Fluid Mechanics*,* Vol. 5, No. 5**,** pp. 481-494.

Furuyama, S., and Chanson, H. (2010). *A Numerical Solution of a Tidal Bore Flow*. Coastal Engineering Journal, Vol. 52, No. 3, pp. 215-234 (DOI: 10.1142/S057856341000218X).

Hornung, H.G., Willert, C., and Turner, S. (1995). *The Flow Field Downstream of a Hydraulic Jump*. Jl of Fluid Mech., Vol. 287, pp. 299-316.

Koch, C., and Chanson, H. (2009). *Turbulent mixing beneath an undular bore front*. Journal of Hydraulic Researc*h*, IAHR, Vol. 47, No. 1, pp. 29-40 (DOI: 10.3826/jhr.2009.2954).

Lighthill, J. (1978). *Waves in Fluids*. Cambridge University Press, Cambridge, UK, 504 pages.

Lubin, P., Chanson, H., and Glockner, S. (2010). *Large Eddy Simulation of Turbulence Generated by a Weak Breaking Tidal Bore*. Environmental Fluid Mechanics, Vol. 10, No. 5, pp. 587-602 (DOI: 10.1007/s10652-009-9165-0).

Montes, J.S., and Chanson, H. (1998). *Characteristics of Undular Hydraulic Jumps. Results and Calculations*. Journal of Hydraulic Engineering, ASCE, Vol. 124, No. 2, pp. 192-205.

Tessier, B., and Terwindt, J.H.J. (1994). *An Example of Soft-Sediment Deformations in an Intertidal Environment - The Effect of a Tidal Bore*. Comptes-Rendus de l'Académie des Sciences, Série II, Vol. 319, No. 2, Part 2, pp. 217-233 (in French).